Reference: *Biol. Bull.* **170:** 211–231. (April, 1986)

SHELL INORGANIC COMPOSITION AND ONSET OF SHELL MINERALIZATION DURING BIVALVE AND GASTROPOD EMBRYOGENESIS[a]

LINDA S. EYSTER[b]

Marine Science Laboratory, Northeastern University, Nahant, Massachusetts 01908

Abstract

Embryos of *Spisula solidissima* (Bivalvia); *Crepidula fornicata, C. convexa, Ilyanassa obsoleta* (Gastropoda: Prosobranchia); and *Dendronotus frondosus, Aeolidia papillosa,* and *Hermissenda crassicornis* (Gastropoda: Opisthobranchia) were reared in the laboratory and examined periodically to determine when shell mineralization began, as detected by birefringence under polarized light. Shell birefringence was detected at preveliger stages in all species. At onset of shell birefringence, samples were prepared for transmission electron microscopy to determine if the transitory shell field invagination (SFI) was still present. Contrary to previous reports for other molluscs, the present ultrastructural evidence indicates that at least for three species studied (*S. solidissima, A. papillosa,* and *H. crassicornis*), the SFI is still present during initial shell mineralization; thus for these three species the cells of the SFI may be involved in initial shell calcification. Electron cytochemical staining with pyroantimonate followed by electron probe microanalysis of thin sections indicated the presence of calcium within the lumen of the SFI in one species (*H. crassicornis*) fixed at onset of shell birefringence. These data suggest that the SFI may play an active role in initial molluscan shell formation. Analysis of veliger shell composition with scanning electron microprobe analysis indicated the variable presence of minor and trace amounts of Na, Mg, Al, P, S, Cl, and K in addition to large amounts of calcium. In two species (*C. fornicata* and *A. papillosa*) shell calcium carbonate was determined by X-ray diffraction analysis to be aragonitic.

Introduction

Molluscan shells consist of both organic matrix materials and inorganic crystalline substances (Wilbur and Saleuddin, 1983). Our current understanding of shell formation in bivalves and gastropods is based primarily on studies of adults or juveniles; very little is known about the formation and composition of molluscan shells prior to metamorphosis. In particular, only a few studies have dealt with the temporal and spatial localization of initial shell mineralization (Fretter and Pilkington, 1971; LaBarbera, 1974). Although embryonic and larval shells are often thought to be calcified (Robertson, 1971; Scheltema, 1971; Thiriot-Quiévreux, 1972; Boltovsky, 1974), the presence of calcium has generally been assumed rather than proven, and the developmental stage at which shell calcification begins within a species has rarely been

Received 22 April 1985; accepted 19 January 1986.

[a] Contribution No. 137 of the Marine Science and Maritime Studies Center, Northeastern University, Nahant, Massachusetts.

[b] Current address: Biology Department, Tufts University, Medford, Massachusetts 02155.

Abbreviations: SFI, shell field invagination; PPA, potassium pyroantimonate.

demonstrated. Because the terms "embryonic shell" and "larval shell" are used differently by different workers, the timing of shell mineralization is often difficult to determine from published reports on the subject.

Fretter and Pilkington (1971) presented histochemical evidence for a lack of mineralization in the larval shells of several marine gastropod species. In non-marine gastropods and in marine gastropods with nurse eggs, calcification is said to take place only after metamorphosis to the juvenile stage (Kapur and Gibson, 1967; Bandel, 1982). Pechenik *et al.* (1984) and Eyster (1985), have recently utilized scanning electron microprobe analysis to demonstrate absence of significant calcification in larval and embryonic shells of the marine prosobranch gastropod *Cymatium parthenopeum* and the opisthobranch gastropod *Coryphella salmonacea* respectively. The degree to which timing of initial shell mineralization varies among taxa remains uncertain, however, partly because of terminological ambiguities and partly because of the false assumption that shell gross morphology can always be used to ascertain presence of shell calcification.

Prior to secretion of the first shell materials during embryogenesis, a portion of the embryonic dorsal ectoderm called the shell field temporarily invaginates, and then evaginates. As development proceeds, these shell field cells multiply and spread over much of the embryonic surface; it is this shell field epithelium that later develops folds or flaps and becomes the mantle (Kapur and Gibson, 1967; Timmermans, 1969; Demian and Yousif, 1973; Kniprath 1977; Shea and Morrill, 1982). The cells of the shell field invagination (SFI: = "shell gland") are generally believed to be responsible for initial shell secretion (*e.g.,* Fretter and Graham, 1962; Jablonski and Lutz, 1980). However, recent ultrastructural evidence from both bivalves and gastropods (Kniprath, 1977, 1980; Eyster, 1983, 1985; Eyster and Morse, 1984b) suggests that the cells of this invagination do not secrete the initial *organic* shell material; instead, the first organic shell material appears to be secreted by shell field cells lying immediately outside the invagination. The role of the invaginated cells in the secretion of early *inorganic* shell materials is unknown. Waller (1978) defined the SFI as the calcifying invagination of the ectoderm, but he did not provide any support for this statement. Moreover, several reports indicate that the SFI is absent at the time of first shell mineralization (Kapur and Gibson, 1967; Kniprath, 1977, 1979, 1981), in which case the invaginated cells can have no active role in initial calcification of the shell.

In the present work several bivalve and gastropod species were studied to determine the stage of development at which shell mineralization was initially detected and then to determine whether the shell field invagination was still present at the onset of shell mineralization. Electron cytochemical stains were utilized in an attempt to localize calcium in relation to the shell field cells at this stage of development. Also reported are the inorganic composition of embryonic and larval shells and the effects of several decalcifying agents.

Materials and Methods

The following species were used in this study: the bivalve *Spisula solidissima,* the prosobranch gastropods *Ilyanassa obsoleta, Crepidula fornicata,* and *C. convexa,* and the opisthobranch gastropods *Dendronotus frondosus, Aeolidia papillosa,* and *Hermissenda crassicornis.* Adults of most species were collected from various locations in Massachusetts, except for *D. frondosus* (from Eastport, Maine) and *H. crassicornis* (from Californian adults; egg masses obtained from Dr. J. Harrigan, Marine Biological Laboratory, Woods Hole, Massachusetts). Because of the small size of the capsules of

the opisthobranchs, embryos of those three species had to be examined and/or treated while still encapsulated.

"Embryo" is used here to refer to all prehatching developmental stages and "larva" refers to all free-swimming stages, as defined by Giese and Pearse (1974). Embryos and larvae of all gastropods were reared from eggs produced naturally in the laboratory. Eggs of the surf clam *Spisula solidissima* were obtained artificially via a gonad-slitting technique (Eyster and Morse, 1984a). All specimens were reared in clean glass dishes of natural seawater maintained under ambient (natural) photoperiods and temperatures.

Polarizing microscopy (pieces of polarizing film set at maximum extinction) was used to ascertain initiation of shell birefringence (see Figs. 1, 16 for examples of birefringent shell material). When the first weak birefringence was observed near the shell field, shell mineralization was said to have begun. That birefringence was due to shell mineralization and not to the shell organic matrix was corroborated by loss of shell birefringence during treatment with decalcifying agents.

Tetracycline was also used in an attempt to identify onset of shell mineralization; tetracycline binds to calcium and produces a fluorescent reaction product (Dey and Bolton, 1973). Embryos were reared in seawater containing tetracycline (50 mg/liter) and were examined periodically with fluorescence microscopy. Although a fluorescent reaction product (indicating shell calcification) was observed, it was not as easy to detect as was the initial birefringence. Therefore, polarizing microscopy rather than tetracycline/fluorescence microscopy was used routinely during this study.

Specimens examined periodically under polarized light were fixed for transmission electron microscopy (TEM) at onset of birefringence to determine if the shell field invagination (SFI) was still present. Standard TEM procedures (glutaraldehyde fixation, osmium-tetroxide post-fixation, ethanol dehydration) were utilized (Eyster, 1983). By necessity, all specimens were sectioned at random orientation.

In an attempt to localize calcium ultrastructurally at onset of birefringence, newly birefringent embryos were incubated either in 0.01–1.0 m*M* naphthaloylhydroxylamine (NHA) in glutaraldehyde (Zechmeister, 1979) or in a 2.5% solution of potassium pyroantimonate (PPA) and osmium tetroxide (Spicer *et al.*, 1968). For unknown reasons the NHA technique failed to produce an electron-dense reaction product even when the shell was known to be calcified, the embryos were incubated without prior glutaraldehyde prefixation, and the NHA concentration was increased two orders of magnitude over that suggested by Zechmeister (1979). The PPA solution was prepared by adding 1 g PPA (Pfaltz and Bauer, Inc.) in 20 ml distilled water; the mixture was heated to near boiling, cooled, reconstituted and mixed 1:1 with 2% osmium tetroxide in 0.3 *M* sucrose (Watabe and Blackwelder, 1980). Embryos and larvae were quickly rinsed with glutaraldehyde to remove sea salts that would precipitate the PPA. Specimens were incubated in the PPA solution for varying lengths of time (0.5–4 h), dehydrated in a graded ethanol series, and embedded in Spurr embedding medium. Sections were collected unsupported on copper grids and examined unstained on an RCA EMU 4 TEM at 50 kV or a Phillips 400 scanning transmission electron microscope (STEM) with an attached energy dispersive X-ray microanalyzer. Analyses of regions with reaction product and regions free of obvious reaction product were conducted for 100 seconds at 40 kV accelerating voltage.

The elemental (Na to Au) compositions of intact shells were determined with scanning electron microprobe analysis. Analyses were conducted with an AMR 1000A scanning electron microscope equipped with a Kevex detector and a Tracor Northern energy dispersive X-ray analyser. For all analyses the stub was set at an angle of 45° to the detector and an accelerating voltage of 20 kV was used. The electron beam was

focused onto random locations on the outer shell surface for all specimens. By analyzing the wavelengths of the element-specific X-rays emitted, it was possible to identify the elements present in each of the probed regions for each shell (Goldstein *et al.*, 1981). The Bremsstrahlung background was subtracted and the total number of counts in each major elemental peak was integrated by computer.

Healthy, active individuals of *Spisula solidissima, Crepidula fornicata, C. convexa, Aeolidia papillosa,* and *Hermissenda crassicornis* were prepared for analysis of shell elemental composition. For several reasons, the specimens selected for elemental analysis had to be older (veligers) than the specimens used elsewhere in this study (trochophores). For microprobe analysis I wanted more shell material than was available at onset of shell mineralization. Also, for the opisthobranch gastropods, I had to use larvae (newly hatched) because the embryos were surrounded by tiny capsules, which could not be removed manually. Both air-dried and critical point dried specimens were prepared. For air-drying, the specimens were rinsed quickly in several changes of distilled water to remove sea salts. For critical point preparations, I exposed veligers to glutaraldehyde fixation, ethanol dehydration, and critical point drying with liquid carbon dioxide. Specimens prepared by both drying techniques were oriented and mounted in known orientation on standard aluminum SEM stubs and were desiccated over silica gel until time of analysis. Shells were not coated prior to analysis.

Additionally, shelled veligers of several opisthobranchs were incubated in 10 m*M* EGTA (ethylene-glycol-bis-N,N-tetraacetic acid) or in calcium-free seawater (CaFSW; calcium replaced with sodium; MBL Supply, Woods Hole, Massachusetts) to examine its effect on shell birefringence and elemental composition of the shell. The egg masses were kept in culture (natural seawater) until hatching was approached or reached. The masses were then cut into two or more pieces and transferred to fresh seawater, EGTA or CaFSW. Experimental details for *Dendronotus frondosus* and *Aeolidia papillosa* are given in the Results section. An egg mass of *Hermissenda crassicornis* was cultured in natural seawater until veligers naturally exited their capsules but had not yet begun to hatch from the gelatinous egg mass. The egg mass was divided into four pieces: C (control) SW-24h (controls in 0.22 μm Millipore filtered seawater for 24 hours), DW-24h (in distilled water, pH = 7.8, for 24 hours), and CaFSW-24h (in CaFSW for 24 hours). The C control shells were prepared immediately for elemental analysis by electron microprobe; shells from the other three groups were prepared for elemental analysis 24 hours later. For all groups, shells were selected and probed at random.

Specimens of *Crepidula fornicata* and *Aeolidia papillosa* were either treated with Feigl's solution (1% silver sulfate in 7.2% manganous sulfate monohydrate) or prepared for X-ray diffraction analysis to determine the crystal morph (calcite *versus* aragonite) in which shell calcium carbonate was deposited prior to hatching. For *C. fornicata,* prehatched veligers removed from capsules of one capsule cluster were used. For *A. papillosa* one egg mass in which embryos had just hatched from their small capsules but not from the egg mass was selected. For both species, the egg mass or capsules were cut open, and the shelled veligers removed, rinsed in several quick changes of distilled water, and transferred onto a glass strip cut from a standard glass microscope slide. As the water was drawn off and evaporated, the shells were pushed with a hair into a closely packed monolayer. No attempt was made to remove body tissues from the shells. Calcium carbonate standards were prepared by powdering aragonite and calcite separately with mortar and pestle, and adding acetone to the powder to produce slurries. These slurries were transferred to separate glass slides. Analyses of crystal morph were made using a Phillips X-ray diffractometer (Cu K_α radiation) with a scan speed of 1°/minute. Intensities of diffracted X-rays were examined from an angle of 20°–60° 2 θ.

RESULTS

The age at onset of shell mineralization for the seven species examined varied from one to fifteen days (after fertilization) depending on the species and the rearing temperature (Table I). However, in all species reported, mineralization of shell organic matrix began in preveliger individuals long before shell-like structures surrounded the young molluscs and long before metamorphosis.

At the time of initial shell mineralization, birefringence was best seen in all gastropod species when the subspherical embryos were oriented (as viewed through the microscope) with the newly secreted shell material lying along the edge of the embryo. When the shell material lay above or below the embryo, the birefringence was often

TABLE I

Initiation of shell mineralization, signalled by onset of shell birefringence. Age is measured from fertilization

Species	Age at onset	Temperature	Comments
Spisula solidissima	33 h	15°c	At 33 h, shell not visible with LM[a] and barely visible with SEM[b].
Crepidula fornicata	9 days	rm. temp. (~20°C)	Day 7: embryos ciliated, moving. Day 9: shell detectable with LM but onset of birefringence variable due in part to presence of runts.
Crepidula convexa	—	—	Youngest available embryos had feet and ciliated vela just forming, and already had strongly birefringent shells that shattered readily under pressure. Shells (140 × 200 μm) still smaller than embryos.
Ilyanassa obsoleta	6 days	rm. temp. (~20°C)	Day 5: first movement observed in some embryos. Day 6: shell birefringence observed in those embryos that had begun to move. Day 7: velar lobes distinct and slightly pigmented; no detected increase in strength of shell birefringence.
Dendronotus frondosus	8 days	8°C	Day 8: most but not all shells birefringent. Shell was capshaped, velum was forming, and statocysts were strongly birefringent (see Fig. 1).
Hermissenda crassicornis	4 days	15°–17°C	Shells of most embryos within egg mass became birefringent over 6 h period. 10 h before birefringence: no embryonic movement and no ciliary movement observed. 7 h before birefringence: cilia first observed.
Aeolidia papillosa	15 days	5°C	Day 13: embryos ciliated, began moving. 4 h after first birefringence: only 10% of shells in mass were birefringent. Day 16: all shells birefringent; shells not visible with LM. Day 18–19: shells were cup-shaped and surrounded posterior halves of embryos.

[a] LM = standard bright field light microscopy.
[b] SEM = scanning electron microscopy.

too weak to be detected through the embryonic yolk. Initial shell birefringence was detected at the onset of embryonic movement, perhaps partly because turning embryos are more likely to be observed in advantageous orientations. Detection of shell birefringence was greatly improved in some species when pressure was applied to the veliger or embryonic capsule until the shell separated from the underlying visceral mass (Fig. 1).

Shell mineralization began when very little organic material was detectable with standard brightfield light microscopy, suggesting mineralization occurs progressively during rather than all at once after formation of the early organic shell. When viewed with shell material on edge at the time of first observed shell birefringence, *Hermissenda crassicornis* embryos had a birefringent region extending one-sixteenth their circumference; the shell was not yet obvious with standard light microscopy, indicating the shell was only a small cap at the time of initial mineralization.

Hermissenda crassicornis is the only species reared in this study that repeatedly had abnormal shell development (see also Hurst, 1967). Single egg masses contained embryos with semi-normal shells, many embryos with long and narrow birefringent shells, and some embryos that lacked birefringent shells but had birefringent statocysts.

The shells of newly hatched larvae of both *Aeolidia papillosa* and *Hermissenda crassicornis* did not collapse upon air drying, suggesting they were either well mineralized or sclerotized; loss of birefringence following treatment with decalcifying agents indicates the shells were mineralized and the lack of shell coloration may suggest the absence of significant sclerotization. As in other nudibranchs, the shells of *Dendronotus frondosus* remained transparent, birefringent, and cracked or shattered under pressure until discarded at metamorphosis. Newly birefringent shells of excapsulated *Crepidula fornicata* embryos deformed when allowed to air day, indicating that they were not heavily mineralized. The shells of excapsulated *C. fornicata* embryos several weeks in age lost their birefringence in 10 m*M* EGTA in about one hour (although at one hour the statocysts were still birefringent).

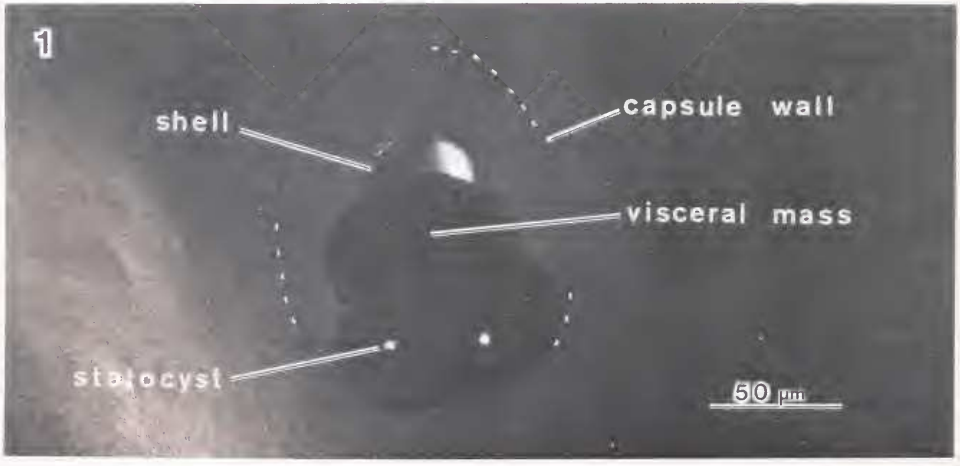

FIGURE 1. Dorsal view of encapsulated 8-day-old embryo of the opisthobranch gastropod *Dendronotus frondosus* observed with polarizing microscopy. To greatly increase visibility of the thin, newly mineralized shell, pressure was applied to the capsule, causing the cap-shaped shell to separate from the underlying visceral mass. Note that both the shell and the statocysts are birefringent.

The SFI at initial shell mineralization

Ultrastructural evidence from three of the above species (*Aeolidia papillosa, Spisula solidissima,* and *Hermissenda crassicornis*) fixed at onset of shell birefringence indicated that the shell field invagination (SFI) was still present when shell mineralization began. In sections through embryos of the opisthobranch *Aeolidia papillosa,* tiny patches ($\sim 1 \times 2$ μm) of microvilli were located between cells about 6–8 μm beneath the embryonic surface and the early organic shell (Figs. 2, 4). By sectioning younger embryos, (23 h before detected shell birefringence), in which the SFI lumen was larger and easier to detect, I was able to locate similar microvillous patches and to confirm that the patch of microvilli was the apparently wider, basal region of the small SFI lumen (Figs. 3, 5). The SFI lumen (in this and the other two species) opened beneath the center of the organic shell cap (Fig. 6); this fact enabled me to locate the very narrow SFI lumen by first locating the extraembryonic shell material. In sectioning through the edge of the SFI in these younger (prebirefringent) embryos, the upper region of the SFI lumen was seen as a narrow channel (Fig. 5). In *A. papillosa* embryos fixed at onset of shell birefringence, no channel was located (Fig. 4), presumably because of sectioning angle rather than absence of the SFI channel.

In the bivalve *Spisula solidissima,* an invagination was seen beneath the small amount of shell material present at first mineralization (Figs. 7, 8). This apparent SFI (the "inner invagination" of Eyster and Morse, 1984a) is narrow (0.5 μm or less wide) and similar to its appearance prior to shell mineralization. Unlike in *Aeolidia papillosa,* no distinct cluster of microvilli was observed lining the SFI lumen.

A narrow SFI channel was detected after onset of shell birefringence in a second opisthobranch, *Hermissenda crassicornis* (Fig. 9). The observed dimensions of this invagination were about 0.5–1.0 μm wide and 10 μm deep (Fig. 10). As in slightly younger embryos fixed prior to shell birefringence, this SFI lumen lay directly under the small cap of organic shell material, as diagrammed in Figure 9.

No SFIs were located at onset of shell mineralization in the other less well studied species. Because the embryos were too undifferentiated to be oriented for sectioning, and because the SFIs had apparently become so narrow, invaginated regions of the shell field were difficult to locate, even in the more well studied species described above.

Specimens of the three species in which an SFI was detected at onset of shell mineralization (*Aeolidia papillosa, Spisula solidissima,* and *Hermissenda crassicornis*) were incubated in an ultracytochemical stain for calcium at the time of initial shell birefringence. Because the quality of ultrastructural preservation is worse with osmium tetroxide—potassium pyroantimonate (PPA) than with standard glutaraldehyde—osmium tetroxide TEM preparations, it was more difficult to locate SFIs in these PPA incubated trochophores. The appearance of the SFIs located in two species are described below.

Larvae of *Spisula solidissima* fixed in osmium tetroxide—potassium pyroantimonate at the onset of shell birefringence showed electron-dense reaction product both inside and outside of shell field cells (Fig. 8) and other cells as well. Scattered granular reaction product was observed throughout the shell field cells of the inner invagination but not in obviously greater density than in non-shell field cells. Reaction product was particularly common over nuclei. In sections through the SFI lumen of one trochophore, a few scattered extracellular clusters of reaction product were seen within the lumen of the invagination; the largest cluster of reaction product was observed extracellularly, in the extrapallial fluid near the pore of the inner invagination (Fig. 8). Because the reaction product was calcium antimonate, as confirmed with

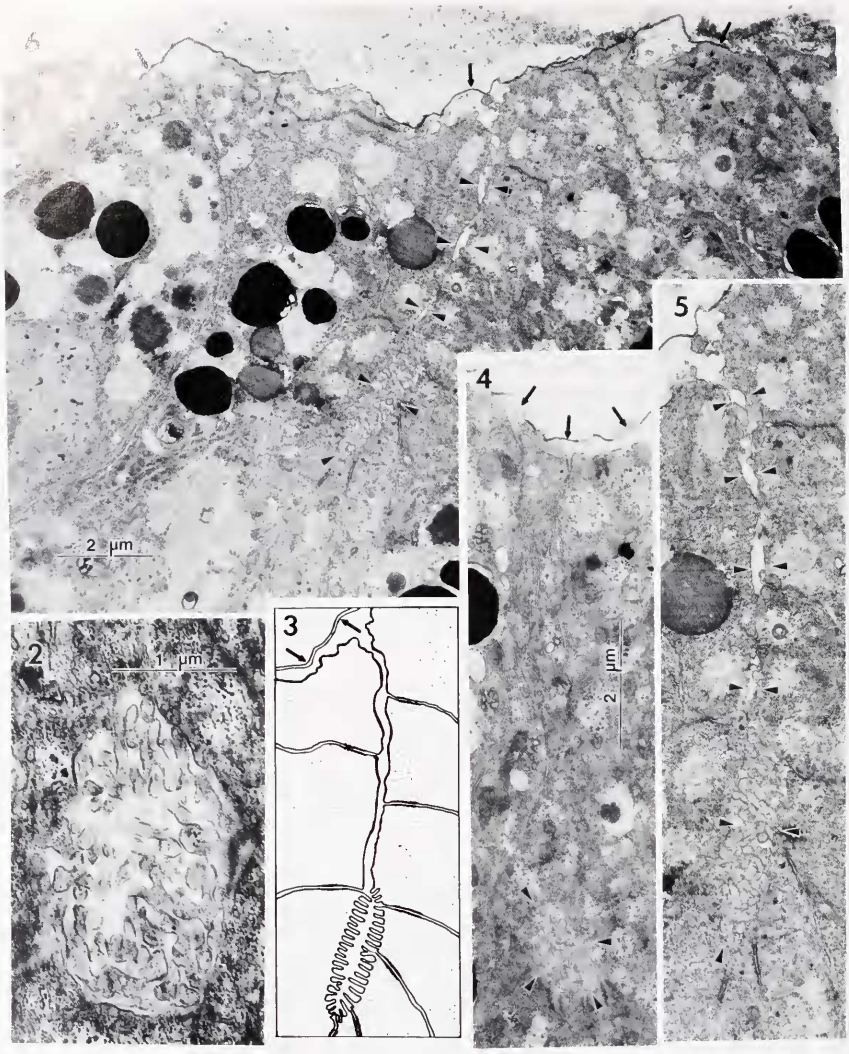

FIGURES 2–6. Sections through shell field cells of the opisthobranch gastropod *Aeolidia papillosa*.

FIGURE 2. Microvillous region believed to be the basal (proximal) region of the SFI lumen detected after the onset of shell mineralization.

FIGURE 3. Schematic diagram of the proposed morphology of the shell field invagination of *A. papillosa* at the onset of shell mineralization. The basal region is lined with microvilli. The distal region is probably canal-like and may be microvillous. The pore of the SFI lumen opens beneath the shell, which at this stage of development consists of two electron-dense layers (arrows). Not to scale.

FIGURE 4. Micrograph showing the inconspicuous microvillous basal region (arrowheads) of the SFI lumen at onset of shell mineralization. The rest of the SFI lumen believed to be present (*i.e.*, a narrow canal connecting the microvillous basal region to the embryonic surface) was not detected. Part of the organic shell (arrows) is visible near the embryonic surface.

FIGURES 5 and 6. Micrographs showing the SFI lumen (arrowheads) at 23 h prior to observation of shell birefringence. The SFI lumen is actually much larger at this stage of development but is shown here in grazing section to demonstrate the similarity between the morphology of its basal region (Fig. 5) and that of the microvillous patch observed 23 h later, at onset of shell birefringence (Fig. 4).

FIGURE 6. Prior to mineralization the organic shell material (arrows) visible along the embryonic surface, isolates the pore of the SFI lumen from the external environment.

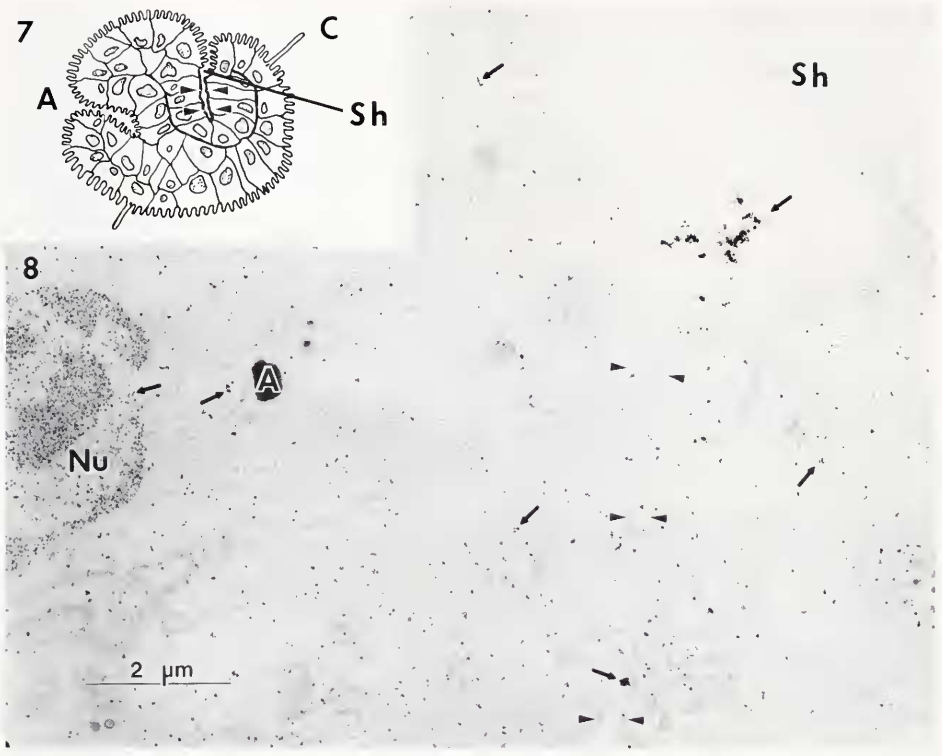

FIGURES 7 and 8. Sections through trochophores (33-h-old) of the bivalve *Spisula solidissima* at onset of shell mineralization. Both figures are in the same orientation. The SFI lumen (arrowheads) was still present.

FIGURE 7. Schematic diagram of section through ciliated (C) trochophore showing two invaginations, the archenteron (A) and the dorsal shell field invagination associated with formation of the early shell (Sh). The small amount of shell material present at this stage would lie at the tip of the pointer and is omitted for clarity. Not to scale.

FIGURE 8. Unstained section through a trochophore fixed in potassium pyroantimonate—osmium tetroxide to localize calcium at onset of shell mineralization. Electron-dense reaction product (arrows) was observed within the shell field cells, extracellularly within the narrow SFI lumen (arrowheads), and clustered at the junction of the SFI pore and the extrapallial space beneath the shell (Sh). Nu = nucleus. A = artifact.

transmission electron microprobe analysis, some calcium may be present in the lumen of the shell field invagination of *Spisula solidissima* during early shell formation.

In one embryo of the gastropod *Hermissenda crassicornis* incubated in PPA, an elongated region consistent with the location and morphology of the SFI was located (Figs, 9, 10). Within this region were large clusters of electron-dense reaction product, in addition to moderately electron-dense material resembling the 'albumen' of the capsular fluid found elsewhere between the embryo and the capsule wall. Within the shell field cells the reaction product was much finer grained (not clumped) than that observed extracellularly. Electron microprobe analysis of reaction product in the lumen of the SFI demonstrated the presence of calcium, as well as antimony and osmium from the fixative. Thus it appears that calcium may be present in the lumen of the shell field invagination of *H. crassicornis* at the onset of shell mineralization.

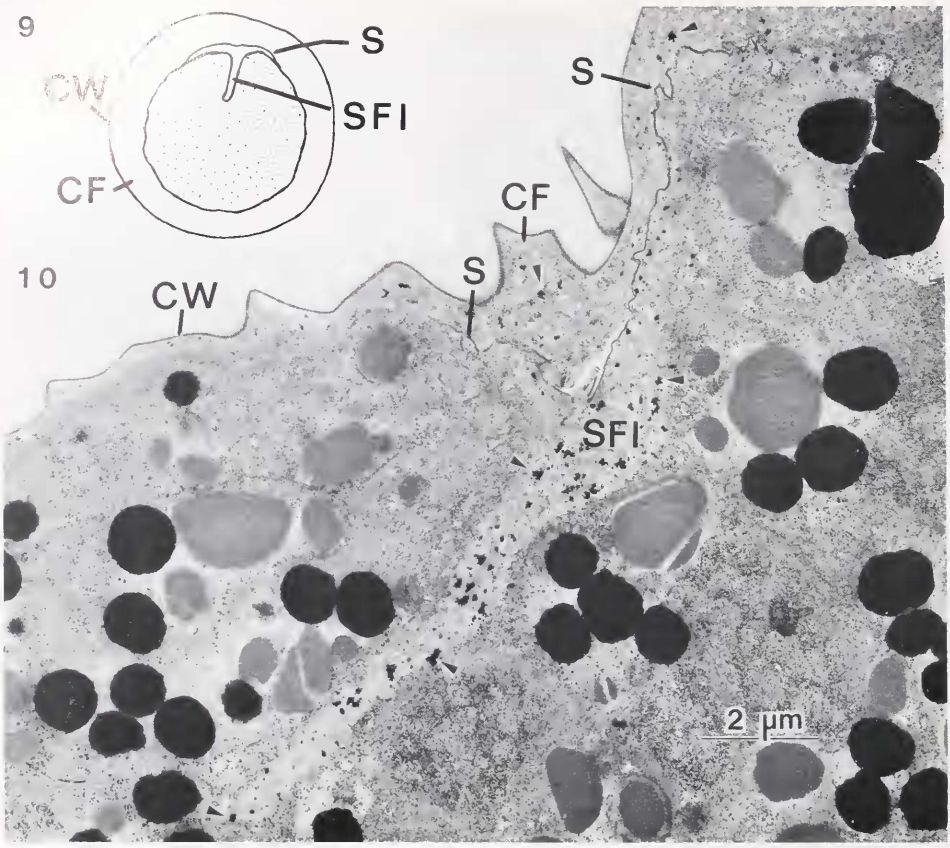

FIGURES 9 and 10. Sections through embryos (4-days-old) of the opisthobranch gastropod *Hermissenda crassicornis* at onset of shell mineralization.

FIGURE 9. Schematic diagram, not to scale, showing shell field invagination (SFI) and shell (S) in same orientation as in Figure 10. The embryo is surrounded by a capsule wall (CW) and the enclosed capsular fluid (CF). For clarity, the capsule is shown elevated from the embryo (as in life), rather than collapsed (as after fixation).

FIGURE 10. Transmission electron micrograph of an unstained section through an embryo, still inside its collapsed capsule (CW), fixed in potassium pyroantimonate—osmium tetroxide at the onset of shell birefringence. The shell field invagination (SFI) was observed beneath the center of the shell material (S). Electron-dense reaction product (arrowheads) containing calcium (and osmium and antimony from the fixative) was observed within the SFI lumen, suggesting calcium may be present in or transported to the SFI lumen during initial shell mineralization. CF = precipitated components of the capsular fluid.

Ultrastructure of newly mineralized shell

At initiation of mineralization, the ultrastructure of the embryonic shell material remaining after standard aqueous TEM preparation appeared identical to its ultrastructure prior to mineralization. In both *Aeolidia papillosa* and *Hermissenda crassicornis* the newly mineralized organic matrix in section appeared as two similar electron-dense layers separated by an electron lucent zone, as diagrammed in Figure 3; it is unclear if this bilayer represents any or all of the periostracum. In newly mineralized shell of *Spisula solidissima* no obvious shell layers or compartments were observed.

The outer shell surfaces of several species were examined with SEM prior to mi-

croprobe analysis of shell elemental composition. For all nudibranch species examined, the larval shells lacked any sculptural pattern or obvious surface microstructure except for a series of raised lines near the aperture, as reported by Hurst (1967) (see Figs. 15, 17). SEM images of broken edges of air-dried *Aeolidia papillosa* larval shells did not reveal any crystalline microstructure, perhaps due to fracture mechanics (O'Neill, 1981). SEM of the shell surface of newly birefringent embryonic shells of *Crepidula fornicata* did not demonstrate any of the calcareous concretions described by Fretter and Pilkington (1971).

Shell composition and decalcification

Electron microprobe analysis of shell elemental composition (Na to Au) indicated that the shell mineral consisted almost entirely of calcium. Figures 11–13 show typical elemental spectra for probes of external shell surfaces. Untreated shells of most species generated large calcium peaks, with much smaller peaks for Na, Mg, Al, P, S, Cl, and K variably present (Table II). Of the non-calcium elements detected, chlorine was the most abundant and the most common. The concentration of each element, including calcium, was highly variable even from one location to another in a single shell, as demonstrated by standard deviation values (Table II). Based on probes near to and

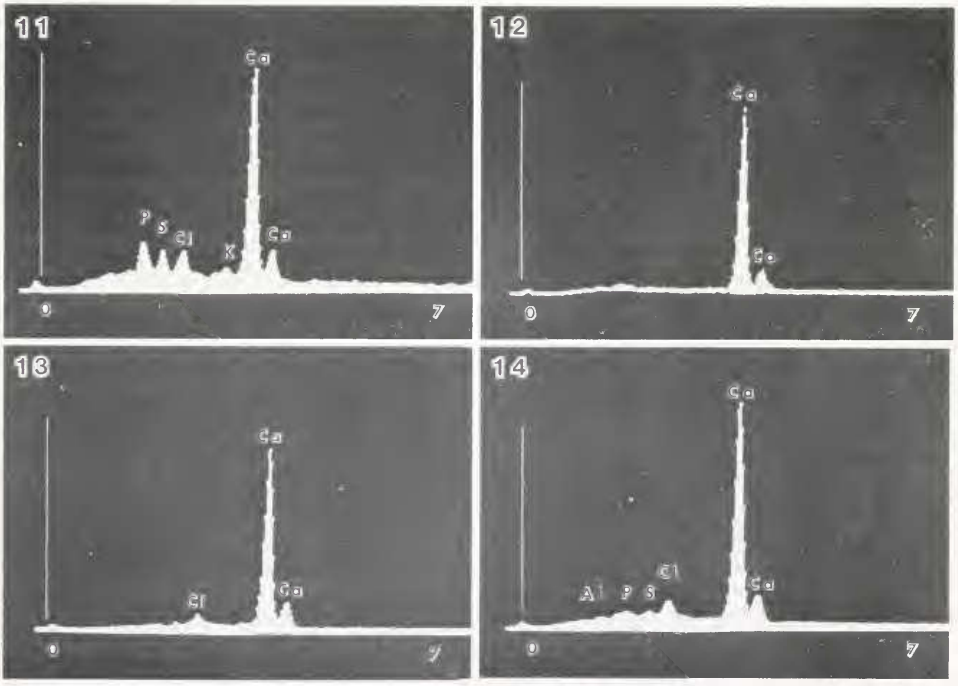

FIGURES 11–14. Typical elemental spectra for shells prior to metamorphosis, demonstrating the presence of calcium for all species. X-ray energy in kiloelectron volts is given on the x-axes. The y-axes, representing the number of X-ray counts, are different for all graphs; to compare amounts of calcium detected see Table II.

FIGURE 11. *Crepidula fornicata.*
FIGURE 12. *Crepidula convexa.*
FIGURE 13. *Aeolidia papillosa.*
FIGURE 14. *Hermissenda crassicornis* reared for 24 h (after hatching) in calcium-free seawater.

TABLE II

Elemental composition (as determined with scanning electron microprobe analysis) of shells of five mollusc species prior to metamorphosis

Species/age, stage or treatment	Elements								N	Shell deformed on air drying
	Na	Mg	Al	P	S	Cl	K	Ca		
Spisula solidissima										
5 day old, 15°C	—	—	—	—	—	0–135	—	3092 ± 668	10	no
Crepidula fornicata										
10 day old[a], rm. temp.	t	t	—	152 ± 45	123 ± 10	294 ± 127	—	1532 ± 221	3	yes
10 day old[b], rm. temp.	—	—	—	182 ± 94	103 ± 33	129 ± 113	t	2313 ± 288	3	yes
Crepidula convexa										
prehatch	—	—	—	—	—	—	t[c]	5160 ± 2700	2	no
Aeolidia papillosa										
control (hatching)	—	—	—	t	—	198 ± 128	—	7571 ± 2075	12	no
into CaFSW in mass, 12d	t	t-180	—	—	144 ± 76	733 ± 216	—	5640 ± 705	6	no
Hermissenda crassicornis										
control (just hatched)	—	—	0–131	0–75	176 ± 64	273 ± 127	t-108	12756 ± 5788	6	no
SW-24h	—	—	66 ± 11	61 ± 4	112 ± 4	331 ± 30	t	12505 ± 2562	2	no
DW-24h	—	—	t	t	103 ± 23	242 ± 43	t	13107 ± 389	2	no
CaFSW-24h	—	—	121 ± 87	106 ± 56	135 ± 75	0–928	t	8853 ± 3385	8	yes

[a] Foot and operculum present, eyes starting to form, shell and statocysts birefringent.

[b] Further developed than [a].

[c] Trace Fe and Zn also detected.

Numbers represent mean ± S.D. N = number of probes. Trace (t) amounts of specific elements were not detected with all probes of one shell or of all shells of one species. Background readings ranged from 5 to 49 (mean ± S.D. = 27 ± 13).

distant from the shell aperture (Gastropoda) or the shell valve edges (Bivalvia), no differences in spatial distribution of the elements were correlated with newly mineralized *versus* older shell material.

Critical point dried shells of some larvae prepared for SEM/microprobe analysis had less calcium than air-dried shells of siblings. In fact, some critical point dried shells became quite wrinkled (Fig. 15), and revealed little or no calcium during electron microprobe analysis. These observations indicate that critical point drying procedures may partially or totally decalcify these lightly calcified samples and should not be used prior to mineral analyses.

The effect of decalcifying agents on shell birefringence and shell elemental composition varied with the decalcifying agent, the animal species, whether or not the animal was alive, and whether or not the animal was within some form of embryonic capsule and/or gelatinous mass. For example, shells of encapsulated *Dendronotus frondosus* veligers (removed from the egg mass) were still highly birefringent after 30 minutes incubation in 10 m*M* EGTA. However, outside of both the gelatinous mass and the egg capsules, the shells of live *D. frondosus* veligers decreased in birefringence within three minutes of incubation in the same solution, suggesting that the egg capsule is an effective barrier to the calcium chelator, EGTA. Also, shells of recently dead *D. frondosus* veligers decalcified more rapidly than did shells of live veligers; empty shells, newly discarded by metamorphosing individuals, decalcified even more rapidly. Shell decalcification was uneven or patchy, suggesting either variable thickness of a uniformly calcified shell or variable distribution of calcification. In shells of living veligers, decalcification was seen first at the aperture lip, perhaps because the new mineral solu-

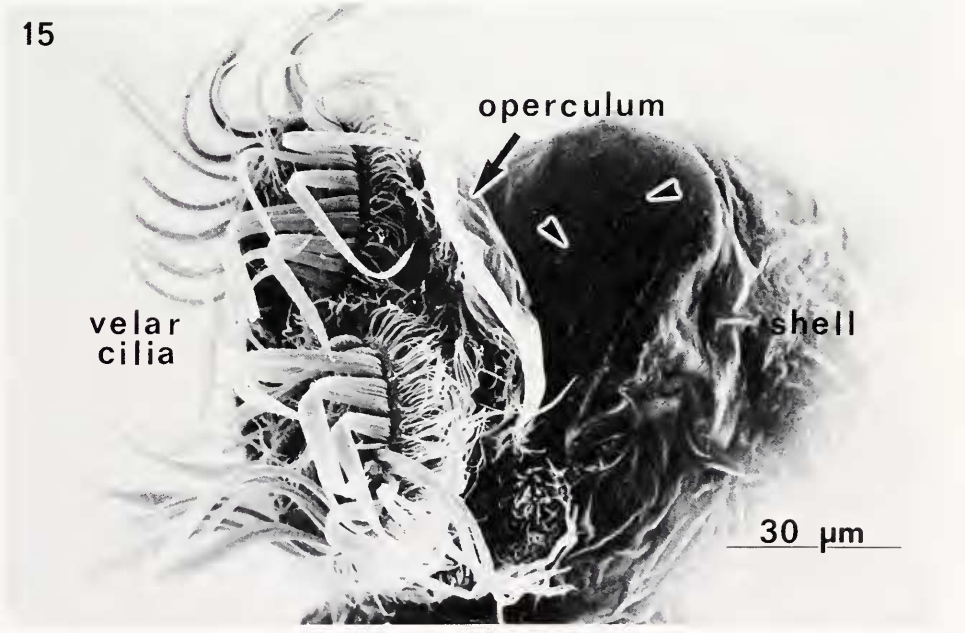

FIGURE 15. Scanning electron micrograph of larva of the opisthobranch gastropod *Aeolidia papillosa*, lying on its dorsal-lateral surface. Raised lines (arrowheads) are visible on the shell near the aperture. The shell is wrinkled because it decalcified during critical point drying procedures, which must be avoided prior to analysis of shell mineralization.

bilized easiest (see Akberali, 1980), because the shell was unprotected internally by living tissue, or because this newly formed region is thinner. Shells of living veligers that were decalcified in EGTA and transferred back to control seawater were not remineralized by 48 hours, but were still a cohesive unit that was collectable by pipette. Shells of recently dead *D. frondosus* veligers left in static distilled water for two weeks or in seawater for two months decalcified but retained their shell shape. Although the organic shell remaining after decalcification retained its shape in static culture, it was flexible and readily collapsed when maneuvered.

For well-developed, encapsulated and enmassed *Aeolidia papillosa* veligers, incubation in CaFSW altered the elemental composition of the veliger shell as well as prolonged the duration of the prehatch period, and reduced by half the number of veligers that eventually hatched. By Day 12 of incubation all veligers maintained in normal seawater had hatched, swam upwards, became caught in the water surface, and died; all veligers subjected to CaFSW were also dead but their shells were opaque rather than transparent and, if hatched, were lying on the dish bottom rather than being stuck at the water surface. Unlike control shells, the opaque shells of treated individuals had detectable amounts of magnesium and sulfur (Table II). There was an obvious decrease in calcium levels in experimental shells.

Incubation of newly hatched *Hermissenda crassicornis* veligers in CaFSW for 24 h also decreased shell calcium compared to that of controls. Control shells, even those trapped in the water surface, were birefringent (Fig. 16) and did not collapse upon air drying (Fig. 17). Inexplicably, entrapment in the water surface was associated with increased decalcification in CaFSW treatments. Shells of free-swimming treated larvae deformed visibly on air drying (Fig. 18), indicating partial decalcification. Other veligers in the CaFSW-24h treatment became trapped in the surface film, and although alive, completely lost shell birefringence; their shells, when allowed to air dry, totally collapsed (Fig. 19), indicating total shell decalcification. Their statocysts, surrounded by body tissues, were still birefringent after 24 hours.

Treatment of *Aeolidia papillosa* veligers with Feigl's solution resulted in the appearance of scattered clusters of black precipitate on the shell surface within five minutes, suggesting that the calcium carbonate of the shell is present as aragonite rather than calcite. X-ray diffraction patterns were obtained for premetamorphic shells of *Aeolidia papillosa* (Fig. 20) and *Crepidula fornicata*. These patterns resembled those obtained from X-ray diffraction of a powdered aragonite standard, demonstrating that the veliger shells for both species were aragonitic.

Discussion

Timing of initial shell mineralization

Gastropod species seem to differ in the timing of initial shell mineralization. In the present paper, shell mineralization began in all species at the trochophore stage of development shortly after the first organic shell material was secreted. In some other species shell mineralization is said to begin later in development. For example, in some marine gastropods that feed on nurse eggs while encapsulated, shell mineralization is delayed (Bandel, 1975, 1982; Rivest, 1983). Teleplanic gastropod larvae may delay abundant shell calcification until after metamorphosis (Pechenik *et al.*, 1984), as an adaptation for long-distance dispersal (Scheltema, 1971). The freshwater gastropod, *Helisoma duryi*, is reported to delay shell calcification until hatching; even a few days after hatching, only occasional crystals of calcium carbonate were observed

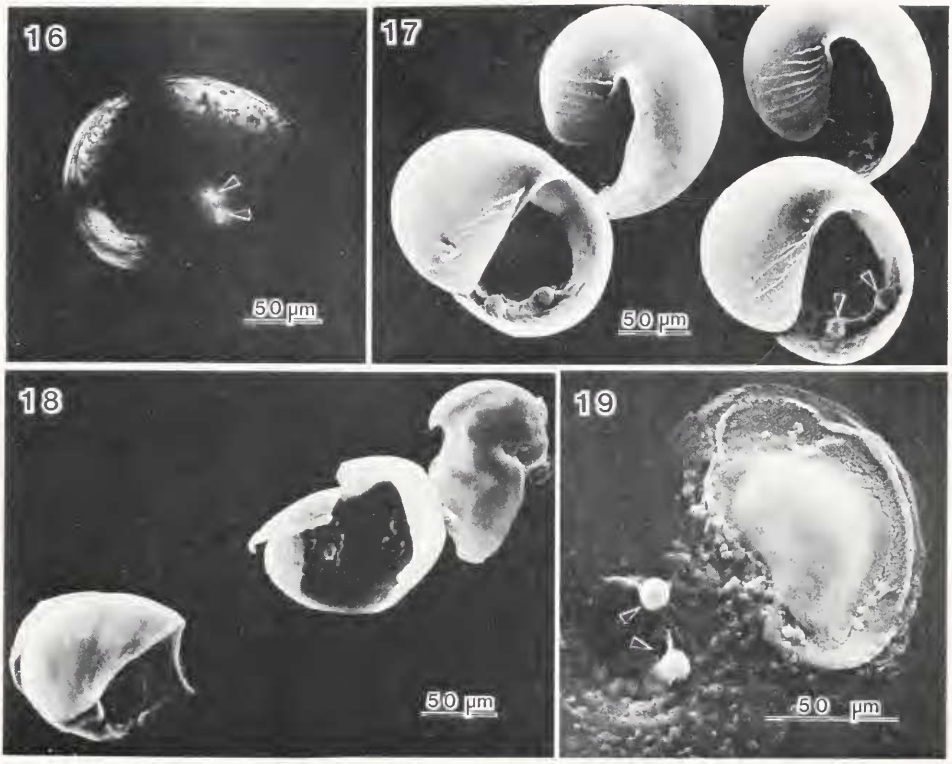

FIGURES 16–19. Shells of newly hatched veligers of the opisthobranch *Hermissenda crassicornis.*

FIGURE 16. Right lateral view of control larva under polarized light, demonstrating birefringence of shell and statocysts (arrowheads). A large portion of the birefringent shell appears dark due to the maltese cross pattern.

FIGURES 17–19. Scanning electron micrographs of air-dried shells.

FIGURE 17. Shells of control larvae. The shells are calcified and show no signs of deformation on air drying. The only shell sculpturing present is a series of raised lines near the aperture. The two spherical structures (arrowheads) visible inside the shell are the statocysts.

FIGURES 18–19. Shells of larvae incubated in calcium-free seawater for 24 h. Shells of swimming larvae were birefringent but deformed during air drying due to partial decalcification (Fig. 18); shells of larvae stuck in the water surface were nonbirefringent, totally decalcified, and collapsed during air drying (Fig. 19). Statocysts (arrowheads) were still birefringent.

in the juvenile shell (Kapur and Gibson, 1967, 1968). In contrast, A. S. M. Saleuddin (pers. comm.) has observed prehatch shell calcification in *H. duryi. Coryphella salmonacea,* a nudibranch gastropod with benthic prejuvenile development, never calcifies its shell (Eyster, 1985); although an organic shell is formed it is not subsequently calcified. Since all nudibranch gastropods shed their shells at metamorphosis, lack of shell calcification by *C. salmonacea* may reflect adaptation to a non-planktonic existence.

According to Fretter and Pilkington (1971), the shells of *Crepidula fornicata* (and of several other prosobranch species) are fibrous, flexible, and do not significantly calcify until metamorphosis. In contrast, the shells of *C. fornicata* veligers observed in the present study were birefringent, shattered under pressure, exhibited prominent

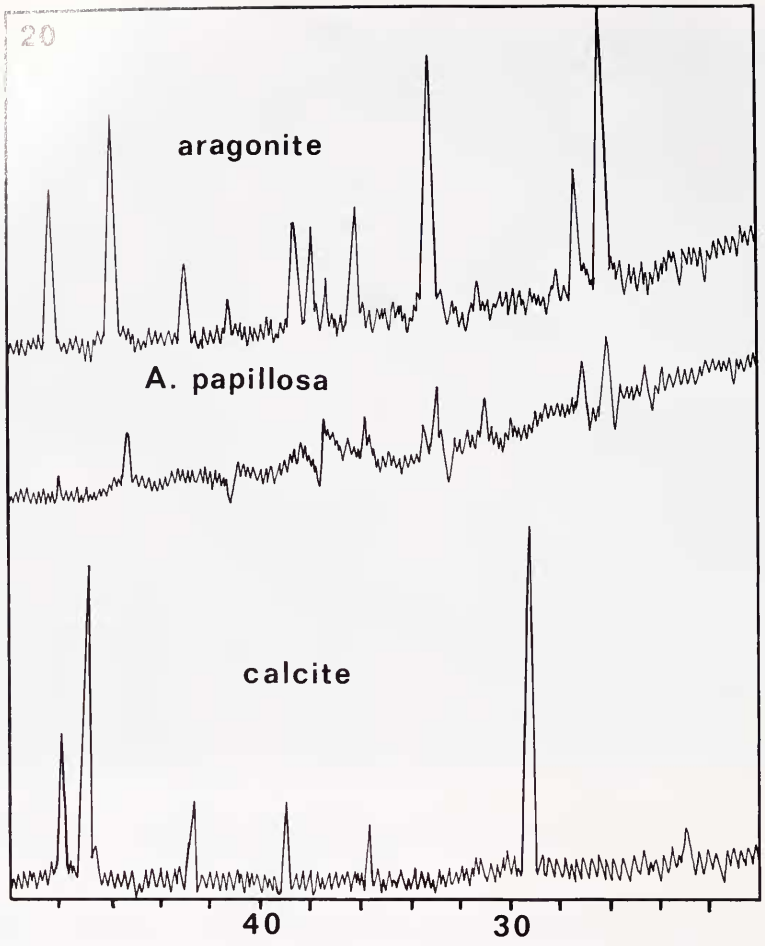

FIGURE 20. X-ray diffraction patterns for aragonite and calcite standards and for shells of recently hatched *Aeolidia papillosa*. Degrees (2θ) are given on the x-axis, for all three samples. Based on peak locations, the calcium carbonate of the shells of *A. papillosa* appears to be aragonitic.

calcium peaks with electron microprobe analysis, and produced peaks indicative of aragonite with X-ray diffraction analysis, all prior to metamorphosis. Clearly more work is required to determine if these apparent intraspecific differences in the timing of shell calcification reflect subtle taxonomic or geographic variation or perhaps differences in environmental conditions.

The early shell of *Crepidula fornicata* veligers was the least calcified of all species examined in the present study. The amount of calcium detected with the electron microprobe was lowest for this species and this is the only species in which untreated shells visibly deformed during air drying. In comparison, the shells of the congener *C. convexa* seemed to be more heavily calcified. The more lightly calcified shell in *C. fornicata* and the more heavily calcified shell in *C. convexa* probably reflect adaptations to presence of a larval stage in the former and the absence of a free-swimming stage in the latter.

Observations in the present study agree with previous reports (Cather, 1967; Ivester, 1972; Tompa, 1973) that mineralization of the shell of *Ilyanassa obsoleta* begins before hatching of the veliger larva. However, no TEM information is available on the morphology of the shell field at the onset of shell mineralization.

Onset of calcification among the Bivalva may be less variable than among the Gastropoda, but whether this is a real difference or is due to an insufficient number of studies on the subject remains to be seen. As pointed out by Waller (1981), the structure of the SFI and of the earliest formed shell is still one of the most poorly known aspects of bivalve larval morphology. The only study to detail the pattern of Prodissoconch I (= first shell) calcification was published in 1974 by LaBarbera. He reported that calcification began before the organic Prodissoconch I was completed, with mineralization beginning at the hinge and proceeding along the shell valve margins before progressing into the center of each valve.

It is not always possible to determine with light microscopy whether embryonic or larval shells are mineralized. For example, the transparent birefringent shells of larval *Hermissenda crassicornis* were mineralized (present study) while the transparent birefringent shells of larval *Cymatium parthenopeum* were not significantly calcified (Pechenik *et al.*, 1984). It is even more hazardous to guess whether shells depicted in the literature are (or were) mineralized. Belisle and Byrd (1980) published SEM micrographs of a *Thais haemastoma* developmental series. They did not mention whether the embryonic shell was calcified (it was not relevant to their study) but after looking at their Figures 32–33 the reader can probably safely conclude that the wrinkled shell is not calcified; however, the reader cannot tell whether the shell decalcified during fixation—critical point drying procedures or was not yet calcified.

It would be helpful if future reports on initial shell mineralization would describe how presence of calcium was demonstrated and describe the developmental stage of the mollusc, rather than only saying that shell mineralization "begins early" or referring to mineralization of the "embryonic shell" or the "larval shell." In the present work, initial shell mineralization was confirmed with a combination of polarizing microscopy, decalcifying agents, tetracycline incubation followed by fluorescence microscopy, electron cytochemical staining followed by transmission electron microprobe analysis, X-ray diffraction analysis, and scanning electron microprobe analysis; shell mineralization began in early trochophores (no mantles, no vela, no feet, no eyes) near the time of onset of ciliary activity. This is not to imply any causal relationship between onset of ciliary movement and shell calcification but to inform future workers of how developed the newly mineralized molluscs were in the present study.

Shell composition

Although the concentration and distribution of shell constituents have been examined in juvenile and adult molluscs (Rosenberg, 1980; Russell-Hunter *et al.*, 1981; Mackie and Flippance, 1983) little is known about the elemental composition of the shells of molluscs prior to metamorphosis. Electron microprobe analysis of the shells of newly hatched veligers of the opisthobranch gastropod *Coryphella verrucosa* revealed only calcium (Eyster, 1985). For veligers of the prosobranch gastropod *Cymatium parthenopeum* collected from the mid-Atlantic Ocean, Al, P, S, Cl, and low levels of Ca were reported from shell surface probes (Pechenik *et al.*, 1984).

The present study has demonstrated that large amounts of calcium and variable amounts of Na, Mg, Al, P, S, Cl, and K are detectable in the shells of some bivalve,

prosobranch and opisthobranch molluscs long before metamorphosis. All of these elements have been previously reported in shells of postmetamorphic molluscs (Nicol, 1967; Carriker *et al.*, 1982; Roesijadi and Crecelius, 1984). Although chlorine was detected in most shells in the present study, it is not clear whether this element is an integral part of the shell or whether chlorine is an artifact from the sodium chloride of the seawater. The absence of a related sodium peak supports the suggestion that the chlorine is a true component of the shell, although sodium is near the detection limit of the equipment utilized. Aluminum has been previously reported from shell analyses of both premetamorphic (Pechenik *et al.*, 1984) and postmetamorphic molluscs (Nicol, 1967; Carriker *et al.*, 1982; Roesijadi and Crecelius, 1984). The facts that this element was not detected in all species in the present study and that probes of the tape between the aluminum stub and the shells did not give aluminum peaks support the supposition that the aluminum is part of or adsorbed to the shell. Sulfur previously has been reported present in shells of juvenile *Mytilus edulis* in the form of $SrSO_4$ and $BaSO_4$ (Travis, 1968), and in the insignificantly mineralized shell of *Cymatium parthenopeum*, possibly as a component of the sclerotized organic matrix (Pechenik *et al.*, 1984). However, in electron microprobe analyses of whole shells, it is impossible to ascertain whether the sulfur is an integral component of the organic matrix, the inorganic mineral, or both. As in shells of adult molluscs, there is no clear-cut distribution of these minor and trace elements within the early shell. It has been hypothesized (Carriker *et al.*, 1983) that the heterogeneous distribution of these elements results from incorporation of detritus into the shell during formation.

The present preliminary experiments involving exposure of veligers to calcium-free seawater (CaFSW) suggest that in the short term absence of environmental calcium some elemental substitution may occur. For example, magnesium was noted in all experimental *Aeolidia papillosa* shells but in no control shells. The alteration of shell elemental composition in even a few shells dried by critical point techniques is sufficient to make it clear that samples used in elemental analyses must instead be air dried, if at all possible. This is true even for lightly calcified shells that may deform or collapse during air drying. The shell decalcification observed in the present study during critical point drying must be attributable to one or more of the fixation/dehydration agents, but why it occurred in some preparations and not in others is unknown.

Role of the shell field invagination (SFI) in shell mineralization

Although for decades the transitory shell gland or invagination of the shell field of molluscs has been said to secrete the embryonic shell, no one has demonstrated that this structure actually secretes any of the organic or the inorganic shell components. Recent ultrastructural evidence argues against a role for the SFI in secreting the first *organic* shell materials (Kniprath, 1977, 1980; Eyster, 1983, 1985; Eyster and Morse, 1984b) and several studies have reported disappearance of the SFI prior to initial shell mineralization (Kapur and Gibson, 1967; Kniprath, 1977, 1980). Although current thinking leans toward support of the century old suggestion (see Kniprath, 1981 for review) that the shell field invaginates solely to bring in proximity the ring of cells that are capable of producing the first organic shell material, the present study provides the first ultrastructural evidence that the invagination of the shell field is still present during and may be involved in shell mineralization. Because shell mineralization may begin even before it is detectable with polarizing microscopy, the invagination may well be present during initial mineralization in more species than reported in this

work. The absence of an SFI in sections of the less well studied species examined here (and in other species in the literature) does not prove that the SFI disappeared by the time shell mineralization began since all SFIs observed to date are extremely narrow and difficult to locate at this stage of development. More detailed studies are needed to determine whether the invagination is really absent at the onset of shell mineralization in any species, because if the SFI is absent, it can not play an active role in initial shell mineralization.

The present electron cytochemical localization of calcium in *Hermissenda crassicornis* embryos suggests that calcium might be transported through cells lining the shell field invagination, to the SFI lumen, and then to the inner surface of the newly formed shell organic matrix. If this pathway is correct, then the invaginated cells of the shell field would be actively involved in initial shell mineralization. However, the calcium localized in the SFI lumen in this study may have been transported there as an artifact of aqueous fixation. Also, the calcium may have entered the SFI lumen via the contiguous extrapallial fluid outside the lumen rather than through the cells of the SFI. Even if future investigations can demonstrate perhaps with ^{45}Ca, that calcium does exit the shell field cells during the invaginated stage, such evidence will not explain why an SFI develops. It is not obvious why a pocket of calcium-rich fluid in addition to the extrapallial fluid present at this and all later stages of shell formation would be beneficial during the initial stages of shell mineralization.

ACKNOWLEDGMENTS

I acknowledge Dr. Malcolm Hill (Earth Sciences Dept., Northeastern University) for assistance with X-ray diffraction analyses; Dr. Alan M. Kuzirian (N.I.H. Biophysics Lab, MBL, Woods Hole) for transmission electron microprobe analyses; Drs. Wm. J. Landis (Harvard Medical School and Children's Hospital) and Jan A. Pechenik (Tufts University) for useful discussions and comments on the manuscript; Len Sudenfield (M.I.T.) for scanning electron microprobe analyses; and Dr. Robert M. Woollacott (Harvard University) for generous access to his ultramicrotome.

LITERATURE CITED

AKBERALI, H. B. 1980. Calcium uptake and dissolution in the shell of *Scrobicularia plana* (da Costa). *J. Exp. Mar. Biol. Ecol.* **43**: 1–9.

BANDEL, K. 1975. Embryonalgehause karibischer Meso- und Neogastropoden (Mollusca). *Abh. Akad. Wiss. Litl math-naturwiss. Kl.* **1975**(1): 1–133.

BANDEL, K. 1982. Morphologie und Bildung der fruhontogenetischen Gehause bei conchiferen Mollusken. *Facies* **7**: 1–198.

BELISLE, B. W., AND W. BYRD. 1980. *In vitro* egg activation and maturation, and ultrastructural analysis of development in the marine prosobranch, *Thais haemastoma*. *Trans. Am. Microsc. Soc.* **99**: 111–127.

BOLTOVSKOY, D. 1974. Study of surface-shell features in Thecosomata (Pteropoda: Mollusca) by means of scanning electron microscopy. *Mar. Biol.* **27**: 165–172.

CARRIKER, M. R., C. P. SWANN, AND J. W. EWART. 1982. An exploratory study with the proton microprobe of the ontogenetic distribution of 16 elements in the shell of living oysters (*Crassostrea virginica*). *Mar. Biol.* **69**: 235–246.

CARRIKER, M. R., C. P. SWANN, AND R. S. PREZANT. 1983. Heterogeneous distribution of trace and minor elements in shell of the oyster, an hypothesis. *Am. Malacol. Bull.* **1**: 102.

CATHER, J. N. 1967. Cellular interactions in the development of the shell gland of the gastropod, *Ilyanassa*. *J. Exp. Zool.* **166**: 205–224.

DEMIAN, E. S., AND F. YOUSIF. 1973. Embryonic development and organogenesis in the snail *Marisa cornuarietis* (Mesogastropoda: Ampullariidae). IV. Development of the shell gland, mantle and respiratory organs. *Malacologia* **12**: 195–211.

DEY, N. D. AND E. T. BOLTON. 1973. Tetracycline as a bivalve shell marker. *Proc. Natl. Shellfish Assoc.* 63: 77.
EYSTER, L. S. 1982. Embryonic shell formation in the nudibranch *Aeolidia papillosa*. *Am. Zool.* **22:** 981.
EYSTER, L. S. 1983. Ultrastructure of early embryonic shell formation in the opisthobranch gastropod *Aeolidia papillosa*. *Biol. Bull.* **165:** 394–408.
EYSTER, L. S. 1985. Origin, morphology and fate of the nonmineralized shell of *Coryphella salmonacea*. *Mar. Biol.* **85:** 67–76.
EYSTER, L. S., AND M. P. MORSE. 1984a. Development of the surf clam (*Spisula solidissima*) following exposure of gametes, embryos, and larvae to silver. *Arch. Environ. Contam. Toxicol.* **13:** 641–646.
EYSTER, L. S., AND M. P. MORSE. 1984b. Early shell formation during molluscan embryogenesis, with new studies on the surf clam, *Spisula solidissima*. *Am. Zool.* **24:** 871–882.
FRETTER, V., AND A. GRAHAM. 1962. *British Prosobranch Molluscs. Their Functional Anatomy and Ecology.* Bartholomew Press, Dorking, Great Britain. 755 pp.
FRETTER, V., AND M. C. PILKINGTON. 1971. The larval shell of some prosobranch gastropods. *J. Mar. Biol. Assoc. U. K.* **51:** 49–62.
GIESE, A. C., AND J. S. PEARSE. 1974. *Reproduction of Marine Invertebrates I. Acoelomate and Pseudocoelomate Metazoans.* Academic Press, New York. 546 pp.
GOLDSTEIN, J. I., D. E. NEWBURY, P. ECHLIN, D. C. JOY, C. FIORI, AND E. LIFSHIN. 1981. *Scanning Electron Microscopy and X-ray Microanalysis. A Text for Biologists, Materials Scientists, and Geologists.* Plenum Press, New York, 673 pp.
HURST, A. 1967. The egg masses and veligers of thirty northeast Pacific opisthobranchs. *Veliger* **9:** 255–288.
IVESTER, M. S. 1972. Ultrastructural study of larval shell formation in *Nassarius obsoletus*. *Am. Zool.* **12:** 717.
JABLONSKI, D., AND R. A. LUTZ. 1980. Molluscan larval shell morphology. Ecological and paleontological applications. Pp. 323–377 in *Skeletal Growth of Aquatic Organisms,* D. C. Rhoads and R. A. Lutz, eds. Plenum Pub. Co., New York. 750 pp.
KAPUR, S. P., AND M. A. GIBSON. 1967. A histological study of the development of the mantle-edge and shell in the freshwater gastropod, *Helisoma duryi eudiscus* (Pilsbry). *Can. J. Zool.* **45:** 1169–1181.
KAPUR, S. P., AND M. A. GIBSON. 1968. A histochemical study of the development of the mantle-edge and shell in the freshwater gastropod, *Helisoma duryi eudiscus* (Pilsbry). *Can. J. Zool.* **46:** 481–491.
KNIPRATH, E. 1977. Zur Ontogenese des Schalenfeldes von *Lymnaea stagnalis*. *Wilhelm Roux's Arch.* **181:** 11–30.
KNIPRATH, E. 1979. The functional morphology of the embryonic shell-gland in the conchiferous molluscs. *Malacologia* **18:** 549–552.
KNIPRATH, E. 1980. Larval development of the shell and the shell gland in *Mytilus* (Bivalvia). *Wilhelm Roux's Arch.* **188:** 201–204.
KNIPRATH, E. 1981. Ontogeny of the molluscan shell field: a review. *Zool. Scri.* **10:** 61–79.
LABARBERA, M. 1974. Calcification of the first larval shell of *Tridacna squamosa* (Tridacnidae: Bivalvia). *Mar. Biol.* **25:** 233–238.
MACKIE, G. L., AND L. A. FLIPPANCE. 1983. Intra- and interspecific variations in calcium content of freshwater Mollusca in relation to calcium content of the water. *J. Moll. Stud.* **49:** 204–212.
NICOL, J. A. C. 1967. *The Biology of Marine Animals.* Sir Isaac Pitman and Sons, Ltd., London. 699 pp.
O'NEILL, P. L. 1981. Polycrystalline echinoderm calcite and its fracture mechanics. *Science* **213:** 646–648.
PECHENIK, J. A., R. S. SCHELTEMA, AND L. S. EYSTER. 1984. Growth stasis and limited shell calcification in larvae of *Cymatium parthenopeum* during trans-Atlantic transport. *Science* **224:** 1097–1099.
RIVEST, B. R. 1983. Development and the influence of nurse egg allotment on hatching size in *Searlesia dira* (Reeve, 1846) (Prosobranchia: Buccinidae). *J. Exp. Mar. Biol. Ecol.* **69:** 217–241.
ROBERTSON, R. 1971. Scanning electron microscopy of planktonic larval marine gastropod shells. *Veliger* **14:** 1–12.
ROESIJADI, G., AND E. A. CRECELIUS. 1984. Elemental composition of the hydrothermal vent clam *Calyptogena magnifica* from the East Pacific Rise. *Mar. Biol.* **83:** 155–161.
ROSENBERG, G. D. 1980. An ontogenetic approach to the environmental significance of bivalve shell chemistry. Pp. 133–168 in *Skeletal Growth of Aquatic Organisms,* D. C. Rhoads and R. A. Lutz, eds. Plenum Pub. Co., New York.
RUSSELL-HUNTER, W. D., A. J. BURKY, AND R. D. HUNTER. 1981. Interpopulation variation in calcareous and proteinaceous shell components in the stream limpet, *Ferrissia rivularis*. *Malacologia* **20:** 255–266.
SCHELTEMA, R. S. 1971. Larval dispersal as a means of genetic exchange between geographically separated populations of shallow-water benthic marine gastropods. *Biol. Bull.* **140:** 284–322.
SHEA, J. M., AND J. B. MORRILL. 1982. Temporal positioning of the developing mantle edge foreshadows the coiling of shell in the fresh water pond snail *Lymnaea*. *Am. Zool.* **22:** 982.

SPICER, S. S., J. H. HARDIN, AND W. B. GREENE. 1968. Nuclear precipitates in pyroantimonate-osmium tetroxide-fixed tissues. *J. Cell Biol.* **39:** 216–221.

THIRIOT-QUIÉVREUX, C. 1972. Microstructures de coquilles larvaires de prosobranches au microscope electronique a balayage. *Arch. Zool. Exp. Gen.* **113:** 553–564.

TIMMERMANS, L. P. M. 1969. Studies on shell formation in molluscs. *Neth. J. Zool.* **19:** 417–523.

TOMPA, A. 1973. Ultrastructural development of *Ilyanassa*'s shell gland. *Malacol. Rev.* **6:** 58.

TRAVIS, D. F. 1968. The structure and organization of, and the relationship between, the inorganic crystals and the organic matrix of the prismatic region of *Mytilis edulis*. *J. Ultrastr. Res.* **23:** 183–215.

WALLER, T. R. 1978. Formation of a posterodorsal notch in larval oyster shells and the prodissoconch I/II boundary in the Bivalvia. *Bull. Am. Malacol. Union Inc.* **1978:** 55–56.

WALLER, T. R. 1981. Functional morphology and development of veliger larvae of the European oyster, *Ostrea edulis* Linne. *Smithsonian Contr. Zool.* **328:** 1–70.

WATABE, N., AND P. L. BLACKWELDER. 1980. Ultrastructure and calcium localization in the mantle epithelium of freshwater gastropod *Pomacea paludosa* during shell regeneration. Pp. 131–140 in *The Mechanisms of Biomineralization in Animals and Plants*, M. Omori and N. Watabe, eds. Proceedings of the Third International Biomineralization Symposium, Tokai University Press, Tokyo.

WILBUR, K. M., AND A. S. M. SALEUDDIN. 1983. Shell formation. Pp. 235–287 in *The Mollusca. Vol. 4. Physiology Part 1*, A. S. M. Saleuddin and K. M. Wilbur, eds. K. M. Wilbur, editor-in-chief. Academic Press, New York.

ZEICHMEISTER, A. 1979. A new selective ultrahistochemical method for the demonstration of calcium using N,N-naphthaloylhydroxylamine. *Histochemistry* **61:** 223–232.